

# Hand Tracking Interface for Virtual Reality Interaction Based on MARG sensors

Nonnarit O-larnnithipong\*, Neeranut Ratchatanantakit\*, Sudarat Tangnimitchok\*, Francisco Ortega\*\*, Armando Barreto\*

\*ECE Department, Florida International University

\*\*CS Department, Colorado State University

## ABSTRACT

Recent years have seen an accelerated development of Virtual Reality (VR) and Augmented Reality (AR) systems. Through these systems, computers immerse users in a completely artificial environment or in one that is partially based on the user's physical surroundings, but partially created artificially. One primary objective of these systems is to cause the perception of actually "being there" (in the environment created by the computer). However, this perception of full immersion may be weakened by the need to use "unnatural" devices (e.g., game controller) to execute actions within the VR or AR environment. Accordingly, increased interest has emerged in developing mechanisms by which the user could interact with VR and AR environments using natural actions, such as the movements of his/her hands.

**Keywords:** Hand tracking, MARG sensors, Accelerometer, Gyroscope, Magnetometer, Orientation estimation.

**Index Terms:** H.5.2 [User Interfaces]: Input devices and strategies

## 1 INTRODUCTION

Recent interest in mechanisms by which the user could interact with a Virtual Reality (VR) or Augmented Reality (AR) environment using natural actions has led to approaches based on hand movements, as they help preserve the perception of full immersion of the user in the environment, which is one of the key goals of many of these systems [5], [11], [13], [14].

This paper outlines our development of one such system, which uses a module containing infrared cameras and multiple miniature Magnetic, Angular-Rate & Gravity (MARG) sensors placed on a glove, worn by the user. We then describe the experimental evaluation of performance for the system, in the context of a simple 3-D target acquisition task.

The main contributions of the work reported in this paper are:

- a) Provides an outline of the innovative Gravity Vector and Magnetic North Vector (GVMNV) orientation correction algorithm, developed for the use of low-cost Magnetic, Angular-Rate & Gravity (MARG) modules in human-computer interaction applications.
- b) Describes the experiment that was designed and performed to evaluate the real-time implementation of the hand-tracking system in the context of a simple 3-D target acquisition task.
- c) Provides the analysis and interpretation of the experimental results, which confirm that the hand-tracking system described has the potential to facilitate the natural interaction of human subjects with VR and AR environments.

## 2 RELATED WORKS

There have been numerous attempts to develop systems for the real-time tracking of the position, orientation and configuration of the human hand by computer systems.

Some early approaches relied on video analysis techniques, but they frequently lacked robustness against occlusion or self-occlusion as the hand of the user adopts different configurations [9]. Using a glove with AR markers has enabled accurate prediction of gestures based on video. However, as all the markers were on the palm, only palm up manipulations were allowed.

With the commercialization of miniature accelerometers and gyroscopes built as Micro Electro-Mechanical Systems (MEMS), new approaches emerged that pursued the tracking of position and orientation for the hand as a whole and/or the several segments that constitute the hand and its fingers (Proximal phalange, middle phalange, distal phalange) [2] [6].

Some solutions place the MEMS modules on the user's right bicep to track orientation and movement in a virtual search task [3]. This tracked the position of the user well but did not allow for much interactivity.

Other work has been done using MEMS in the form of rings [10], large body sensors [1], and magnetic sensors [7]. When using rings, the system was bulky and only had a limited set of interactions (clicking and drawing) [10]. Using magnetic sensors allowed only limited interactivity. The only implemented object manipulations were pinching and grasping [7].

A processing issue that may occur when MEMS sensors are used is a difficulty in maintaining real-time interactivity. Some of the algorithms used to process the MEMS data add considerable latency to the system [15].

Moreover, MEMS-based accelerometers and gyroscopes have performance characteristics that are much lower than their larger-size, navigation-grade counterparts [4]. Because of this, the tracking of individual accelerometer+gyroscope modules could not be achieved using the same "strapdown" processing techniques as employed for navigational tracking of these Inertial Measurement Units (IMUs). Strapdown IMU processing calls for double integration of the accelerometer signals, once those measurements have been "resolved" (geometrically projected) to fixed coordinate axes on the bases of highly accurate orientation measurements. The higher levels of inaccuracy in the MEMS-based accelerometers and gyroscopes have precluded using a similar approach for hand tracking.

## 3 HAND TRACKING APPROACH

In view of the above, our approach uses an infrared video system, containing 3 cameras (OptiTrack V120 TRIO), for the exclusive purpose of tracking the position of the wrist of the glove, where IR-reflective markers have been placed. This informs the system of the position of the "Wrist-Root" (WR). In

---

\* Email address for N. O-larnnithipong: nolar002@fiu.edu

addition, we propose placing miniature MARG modules (Yost Labs 3-Space) in the back of the glove, and on the proximal and middle phalanges of the fingers of the glove, with the sole purpose of robustly estimating the orientation of these anatomical segments. Given the known length of the hand segments, knowledge of their orientations, along with the WR position, are combined to determine, in real-time, all their positions and orientations. (In the experiments described here only the back of the hand and the distal phalange of just the index finger are instrumented, and tape is applied to the articulation between the middle and the distal phalanges, to make them act as a single, continuous mechanical segment). The MARG and the glove, as instrumented for the experiments described in later sections, appear in Figure 1.

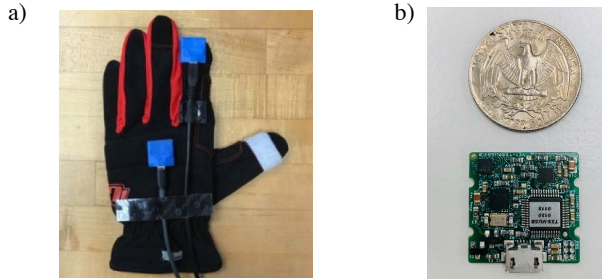


Figure 1: a) Glove with MARG modules attached to the dorsal surface (back) of the hand and to the tip of the index finger. b) Yost 3-Space MARG module next to a US quarter coin.

Even when focusing exclusively on the goal of estimating the orientation of a MARG module attached to a hand segment (e.g., proximal phalange), the performance characteristics of the MEMS MARG sensors represent a significant challenge. In essence, the current orientation of the MARG is estimated as the accumulation of changes in orientation, reported by the 3 gyroscopes in the module, from a known initial orientation (“Dead Reckoning”). However, the gyroscopes in the MARG exhibit (“slowly”) time-varying offsets (“biases”) that, therefore, introduce increasing departures from the true orientation (known as “drift”) as the orientation changes are accumulated by the system.

We have developed a dual correction approach that, in summary, waits until the MARG is static or close-to-static and then:

- a) Uses the current orientation estimate to calculate the projections of initially known vectors (gravity vector, magnetic north vector) on the current directions of the 3 orthogonal sensor axes (accelerometer, magnetometer),
- b) Compares the calculated gravity and magnetic north vectors to the current readings measured from the corresponding sensors (accelerometer, magnetometer),
- c) Obtains a numerical representation (in quaternion form) of the orientation discrepancies between the calculated and measured vectors (gravity vector, magnetic north vector),
- d) Uses the discrepancies to create two versions (accelerometer-corrected and magnetometer-corrected) of the corrected orientation estimates, and
- e) Interpolates between the corrections, according to the operating context of the MARG, to define the final orientation estimate result.

The following paragraphs offer a more detailed outline of the steps referred above.

Our approach includes a continuous estimation of the gyroscope biases, to try to remove them and obtain “unbiased” gyroscope outputs,  $\omega_b$ , but this, in itself, may be insufficient. Therefore, whenever the MARG is static, we perform adjustments (corrections) to the original orientation estimation (in quaternion form),  $q_G$ , by using it to calculate what would be the 3 orthogonal components of the gravity vector (GV) and then comparing it to the actual measurements of the accelerometers at that point in time. The system then calculates an accelerometer-corrected orientation quaternion,  $q_{GA}$ , which breaks down the continuous accumulation of error that would continue to worsen if just the “Dead Reckoning” orientation update (based on just the gyroscope readings) were taking place.

The process followed to obtain the accelerometer-corrected quaternion is defined by the following equations. The uncorrected (dead reckoning) quaternion orientation estimate,  $q_G$ , is found by accumulation of the unbiased gyroscope signals,  $\omega_b$ :

$$\dot{q} = \frac{1}{2} \hat{q}_0 \otimes \omega_B \quad (1)$$

$$q_G = \exp(\Delta t \dot{q} \otimes \hat{q}_0^*) \otimes \hat{q}_0 \quad (2)$$

where the “ $\otimes$ ” represents quaternion product, the “ $*$ ” superscript indicates quaternion conjugation and the dot on top of a quaternion variable represents its derivative with respect to time. (The triangular “hat” is just included to emphasize the fact that the corresponding quantity is an estimate). Then, as this correction takes place when the MARG is not moving significantly, this  $q_G$  is used to calculate the components of gravity in the current directions of the MARG accelerometers (its “Body Frame”), denoted by  $a(q_G)$ , through a change of bases applied to the initial gravity vector in the fixed “Earth Frame”,  $A_{int} = [0, 0, -1]$  (The arrow on a variable emphasizes that it is a 3-D vector, not a quaternion):

$$\vec{a}(q_G) = q_G^* \otimes A_{int} \otimes q_G \quad (3)$$

The orientation difference between  $a(q_G)$  and the actual set of measurements from the 3 accelerometers in the MARG,  $a_b$ , is found, as  $\Delta q_A$ , and then the accelerometer-corrected orientation estimate,  $q_{GA}$ , is found by “appending” (by quaternion product)  $\Delta q_A$  to the original  $q_G$ :

$$\hat{q}_{GA} = q_G \otimes \Delta q_A \quad (4)$$

A more detailed description of the process outlined above to determine  $q_{GA}$  can be found in [12].

The process to find a “magnetic correction quaternion”  $\Delta q_M$ , follows a parallel reasoning, with the exception that now  $M_{int}$ , the vector of initial magnetometer readings, representing the magnetic North Vector (MNV) recorded during initialization of the system, is used instead of  $A_{int}$ . Further, the comparison is now between the calculated projection of the MNV to the body frame,  $m(q_G)$ , and the set of current magnetometer readings,  $m_b$ , to yield the orientation difference quaternion  $\Delta q_M$ . This quaternion is then “appended” to  $q_G$  to obtain the magnetometer-corrected orientation estimate,  $q_{GM}$ . The corresponding equations are:

$$\vec{m}(q_G) = q_G^* \otimes M_{int} \otimes q_G \quad (5)$$

$$\hat{q}_{GM} = q_G \otimes \Delta q_M \quad (6)$$

However, the assumptions for both these corrections may not be fulfilled exactly. The magnetometer correction assumes that the magnetic field vector is constant in the complete environment in

which the system is used. In reality, the presence of large ferromagnetic objects may distort the magnetic field in the space around them. On the other hand, the accelerometer correction assumes that the instantaneous readings from the accelerometer,  $a_n$ , are responding exclusively to the earth's gravity. This is true when the MARG is not moving with significant variations in speed. We use a variable provided by the Yost 3-Space MARG labeled "stillness" ( $\alpha$ ), ranging from 0.0 (strong movement) to 1.0 (no movement at all), to only attempt orientation estimation corrections when  $\alpha$  is close to 1.0. This is appropriate for the hand-tracking context, because humans do not continuously move their hands in an incessant fashion, yielding, therefore, frequent intervals of high stillness when the corrections can be applied. In those cases, the final version of the corrected orientation estimate in quaternion form,  $q_{OUT}$ , is a weighted interpolation between  $q_{GA}$  and  $q_{GM}$ , in which  $q_{GA}$  is favored in proportion to the closeness of  $\alpha$  to 1.0 :

$$\Omega = \cos^{-1}(\hat{q}_{GM} \cdot \hat{q}_{GA}) \quad (7)$$

$$\hat{q}_{OUT} = \frac{\hat{q}_{GM} \sin((1-\alpha)\Omega) + \hat{q}_{GA} \sin(\alpha\Omega)}{\sin(\Omega)} \quad (8)$$

Once  $q_{OUT}$  is calculated, it is used to replace  $q_0$  in the dead reckoning orientation estimation (Eqs. 1 and 2) and the process continues. Because, overall, the correction involves consideration of the gravity vector (GV) and the magnetic north vector (MNV), we will refer to the complete process as the GVMNV orientation correction approach. The position and orientation estimates are applied, in real-time, to animate a prototype virtual hand developed in Unity, where a 3-dimensional target acquisition experiment was set up.

## 4 3-DIMENSIONAL TARGET ACQUISITION EXPERIMENT

### 4.1 Experimental Setup

In order to prove the concept of real-time implementation of the GVMNV orientation correction algorithm used for the hand motion tracking interface, the algorithm was adapted for real-time performance using a C# script within Unity. To evaluate the compatibility of this orientation correction algorithm on the hand motion tracking interface, a game scene (3D environment) in Unity has been created as shown in Figure 2.

The 3-D hand model shown in Figure 2 was attached to the C# scripts that stream the marker position in 3-D space and the raw accelerometer, gyroscope and magnetometer data. The marker position from the OptiTrack V120 TRIO system was assigned as the position of the wrist of the 3-D hand model. The C# script that streams raw accelerometer, gyroscope and magnetometer data also implemented the GVMNV orientation correction algorithm. For every frame of rendering, the output estimated quaternion ( $q_{OUT}$ ) was calculated for the hand, and distal phalange. (If only the proximal and middle phalanges are instrumented, the orientation of the distal phalange can be estimated by using the relationship between the flex angles of the middle and distal phalanges found by Ip and Chan [8].) The quaternion expressions of those orientations were assigned as the rotations for the respective parts of the hand model in Unity.

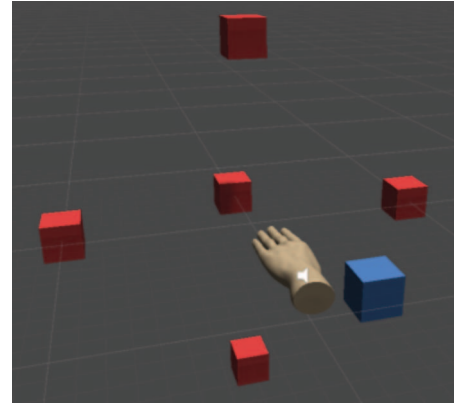


Figure 2: Unity game scene for testing real-time implementation of the orientation

To evaluate the performance of the hand motion tracking interface, a game scene with five red cubes (5 cm. side) and one blue cube (5 cm. side) was created as shown in Figure 2. The experimental subject wore the glove and was asked to acquire all the red cube targets as they appeared in the virtual in 3-D space, which was displayed in front of the subject, in a computer monitor.



Figure 3: Initial Unity scene, where the subject enters his/her ID, prior to the actual experimental tasks.

The experimental sequence is as follows: Initially a blue ("home") cube will appear in the virtual environment. A single red cube will appear in the scene after acquiring the blue cube. The acquisition of the blue cube marks the starting time for the subject to acquire the red cube. The red cubes will appear (one at a time) in 3-D positions that are at the same distance (40 cm.) from the origin, where the blue cube appears. Four of the red cube positions were at +/- 45° elevation or azimuth from the position directly in front of the blue cube location. The time to acquire each red cube was recorded. The blue cube appeared for the first time after the Subject ID was entered, as shown in Figure 3.

In order to acquire each of the cubes in this task, the subject has to flex his/her index finger while colliding with the cube. The 3-D hand model will change its color into green when the flexion of the index finger is detected, as shown in Figure 4. In each acquisition process, after the blue cube is acquired, the red cube

will appear. The subject will then move his/her hand in 3-D space to reach the red cube and flex the index finger to acquire it as shown in Figure 5. After the subject acquires each of the 5 red cubes, the time for that acquisition is recorded. When all 5 cubes have been acquired, the total trial time will be calculated as the sum of the 5 acquisition times.

Five college-aged human subjects (2 females and 3 males) were recruited to participate in the experiment. All five subjects were right-handed.

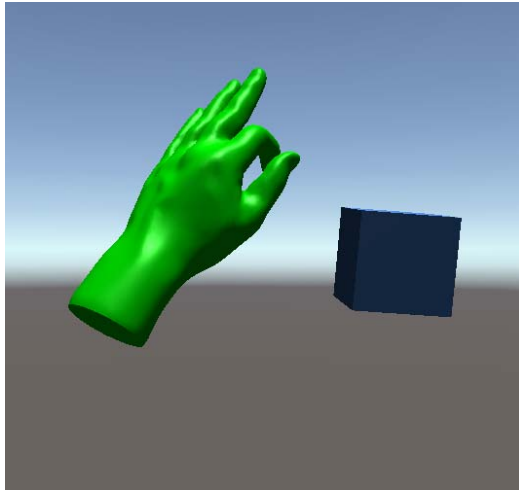


Figure 4: The 3-D hand model will turn into green indicating the state of flexing

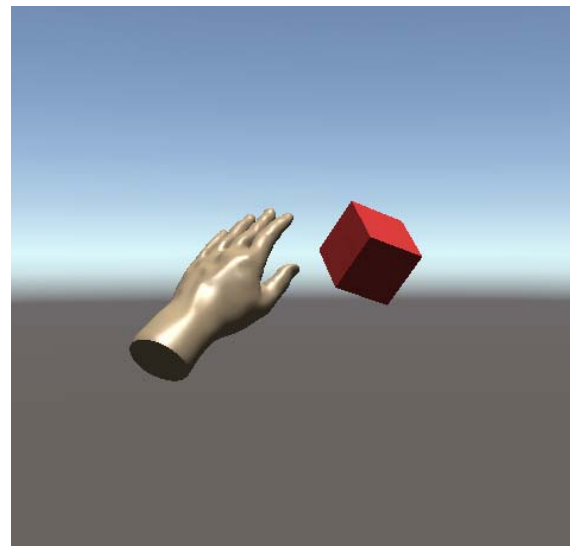


Figure 5: The red cube will appear after acquiring the blue cube.

#### 4.2 Experimental Results and Analysis

The results from the evaluation experiment are summarized in Table 1, below. Five human subjects participated, and each of the subjects completed 2 trials, each one of them consisting of 5 red cube acquisitions.

The table provides detailed timing (on each row) for the acquisition of each of the 5 red cubes during each of the 2 trials performed by each of the 5 subjects. The right-most column provides the total trial times for each trial.

Table 1: Statistical data of the time used to acquire red cubes

Subject No.	Trial No.	Time in seconds					Total Time
		Cube #1	Cube #2	Cube #3	Cube #4	Cube #5	
1	1	4.562	4.896	4.705	5.240	7.828	27.230
	2	4.364	4.324	6.150	2.117	10.651	27.607
2	1	4.626	6.903	10.404	8.236	16.081	46.250
	2	6.078	6.698	6.408	7.141	20.097	46.421
3	1	6.169	8.577	2.693	1.730	4.056	23.226
	2	2.575	10.236	2.560	4.325	1.901	21.598
4	1	2.171	1.750	2.702	5.985	2.127	14.735
	2	2.959	1.836	2.278	2.052	7.572	16.696
5	1	1.398	4.914	1.549	2.496	1.598	11.956
	2	1.161	3.394	3.776	3.309	4.080	15.719
	Mean	3.606	5.353	4.323	4.263	7.599	25.144
	SD	1.813	2.771	2.695	2.308	6.332	12.326
	Min	1.161	1.750	1.549	1.730	1.598	11.956
	Max	6.169	10.236	10.404	8.236	20.097	46.421

## 5 DISCUSSION

Focusing on the mean red cube acquisition times for cubes #1 to #5, we observe that these mean values are all around 5 seconds. As the distance between the home (blue) cube and any of the target (red) cubes was 40 cm, this timing does not seem impractically long. We also notice that cubes #2, #3 and #4 have similar average acquisition times (all close to 5 seconds), with relatively narrow spreads (standard deviations). However, acquisition times for cube #1 are shorter and less variable ( $\mu = 3.606$  s;  $\sigma = 1.813$  s). In contrast, cube #5 has a higher-than-usual mean acquisition value (7.599 seconds) with a much broader spread around that mean ( $\mu = 6.332$  s). It is possible that cube #1 was particularly “easy” to acquire, while cube #5 was particularly “hard” to acquire for the subjects.

Indeed, the cube designated as cube #1 is the one that appeared right in front of the blue cube ( $0^\circ$  azimuth,  $0^\circ$  elevation). Therefore, it was particularly “easy” for most of the subjects to move their hand forward to reach it. Similarly, cubes #2 and #3 were virtually placed in the same horizontal plane (“same height”) as the blue cube, at azimuths of  $-45^\circ$  (i.e., to the left) and  $45^\circ$  (i.e., to the right), respectively. Both of them seem to have been relatively “easy” to acquire. Cubes #4 and #5 appear both in front of the blue cube, but at elevations of  $45^\circ$  (above) and  $-45^\circ$  (below), respectively. It seems, therefore that acquiring the red target cube that appeared below the height of the blue, home cube was more challenging for some of the participants. The specific characteristics of the subjects, of course, introduce some variation within the values in each of the columns of Table 1 (Cube #1, ..., Cube #5) but the trends mentioned above seem to be present across the set of subjects. Nonetheless, the typical acquisition time of about 5 seconds observed confirms that the hand tracking system seems to provide a natural and efficient way for a human subject to interact with a simple virtual environment. (It should also be considered that, as we were mainly interested in evaluating the performance of the hand tracking system as input mechanism, the test used as simple visual feedback to the user the real-time display of the virtual scene on a flat panel computer monitor, which might have challenged the eye-hand coordination of the subjects, during the trials.)

Overall, the experimental results and their analysis, as discussed above, confirm that the hand-tracking system described here has the potential to facilitate the natural interaction of human subjects with VR and AR environments.

The MARG-based hand tracking system depends on the algorithm we have proposed for periodically correcting the orientation estimates obtained from the MARG gyroscope. It should be noted that there is an important characteristic which distinguishes our approach from other “Sensor Fusion” algorithms, such as Kalman filtering. Our mechanisms of orientation correction, based on one hand on the gravity vector and on the magnetic north vector, on the other, are implemented in fully parallel tracks, without comingling these two independent sources of information until the very late stages in which the interpolation takes place to define the final GVMNV-corrected orientation estimate. This characteristic preserves the interpretability of all the parameters on both parallel tracks throughout the process and facilitates the assignment of regulatory parameters (i.e.,  $\alpha$ ) used for the information fusion that takes place in the last stage of the process.

After assessing the initial hand-tracking capabilities that the proposed method seems to provide, it is important to place this approach in the context of other hand-tracking methods. For example, the Microsoft Kinect (V2) module is capable of tracking

the shape and motion of the human body, as exemplified in the “Skeleton Tracker” program. This Kinect capability is based on information captured by Kinect’s RGB video camera and its “Time-of-flight” (depth) sensor. Similarly, the Leap Motion system, based on 2 cameras and 3 infrared LEDs, is capable of tracking hand movements and flexions, while the hands are kept hovering over the device. However, these camera-based approaches are likely to lack robustness in the following aspects:

- They require sustained line-of-sight between the cameras and the fingers and joints.
- They will work better when the fingers are close to the cameras, as their representation in the images will be more conspicuous and the resolution of the quantization of distance (meter/pixel) will be more advantageous (less error).
- They may be negatively impacted by “self-occlusion” if gestures performed by the hand disturb the line of sight between the cameras and some of the fingers and joints.

In contrast, if we considered the use of the approach proposed here with a glove fitted with two MARG sensors on each finger (on the proximal and middle phalanges), and the use of Ip and Chan’s formula [8], we would be able to obtain the orientation information with the same level of accuracy, irrespective of the location of the user. Similarly, the vulnerability of the proposed approach to disruptions in line of sight have been reduced to just the position estimation of the wrist of the glove, which is a larger target for the 3 cameras in the OptiTrack V120 Trio system we have used.

Therefore, we expect that the proposed approach, implemented on a fully instrumented glove, will yield a hand-tracking solution that will be less vulnerable to line-of-sight disruptions and capable of the same level of performance at varying distances. This is in contrast with approaches based on Kinect or Leap Motion sensors, which have an implicit expectation of performance decay with longer distances.

## 6 CONCLUSIONS

This paper has provided a succinct outline of the development of our real-time hand-tracking system, which is based on a small set of infrared video cameras and MARG modules attached on the glove worn by the user. In particular, we have outlined the algorithm used for correcting the orientation estimations provided by the MARG modules on the bases of measurements of the gravity vector and the magnetic north vector. This paper also described the set up of a 3-D target acquisition experiment, involving 5 human subjects, for the purpose of assessing the efficacy of our system for 3-D interaction within a virtual environment.

The results from the evaluation experiment indicate, overall, that the hand-tracking system provides a viable mechanism for a user to interact with a virtual environment. It also seems likely that the performance of the hand-tracking system could improve if a more immersive visualization mechanism (e.g., head-mounted display, Oculus Rift, etc.) were to be used for the evaluation tasks.

## ACKNOWLEDGMENTS

This material is based in part upon work supported by the National Science Foundation under Grant Nos. I/UCRC IIP-1338922, III-Large IIS-1213026, MRI CNS-1429345, MRI CNS-1532061 and the FIU Graduate School Dissertation Year Fellowship awarded to Dr. Nonnarit O-Iarnnithipong. The authors wish to acknowledge the assistance provided by Mr. Adam Williams (CSU), in the preparation of this article.

## REFERENCES

- [1] Eric R. Bachmann, Robert B. McGhee, Xiaoping Yun, and Michael J. Zyda. 2001. Inertial and magnetic posture tracking for inserting humans into networked virtual environments. In Proceedings of the ACM symposium on Virtual reality software and technology (VRST '01). ACM, New York, NY, USA, 9-16. DOI=<http://dx.doi.org/10.1145/505008.505011>
- [2] T. D. Bui and L. T. Nguyen, "Recognizing postures in Vietnamese sign language with MEMS accelerometers," *IEEE sensors journal*, vol. 7, no. 5, pp. 707-712, 2007.
- [3] H. Chien, N. Hu, P. Tsai, T. Wu and J. Chen, "Study on the use of wearable devices to control objects in virtual reality," 2016 International Conference on Advanced Materials for Science and Engineering (ICAMSE), Tainan, 2016, pp. 646-648. doi: 10.1109/ICAMSE.2016.7840268
- [4] E. Foxlin, (2002) "Motion Tracking Requirements and Technologies", Chapter 8 in *Handbook of Virtual Environments: Design, Implementation, and Applications*, pp. 163 – 201. Kay Stanney, Ed., Lawrence Erlbaum Associates.
- [5] C. Heeter, "Being there: The subjective experience of presence," *Presence: Teleoperators and Virtual Environments*, vol. 1, no. 2, pp. 262-271, 1992. doi: 10.1162/pres.1992.1.2.262; 07.
- [6] J. L. Hernandez-Rebollar, R. W. Lindeman, and N. Kyriakopoulos, "A multiclass pattern recognition system for practical finger spelling translation," in *Multimodal Interfaces, 2002. Proceedings. Fourth IEEE International Conference on*, pp. 185-190, IEEE, 2002.
- [7] K. Hirota and K. Tagawa, "Interaction with virtual object using deformable hand," 2016 IEEE Virtual Reality (VR), Greenville, SC, 2016, pp. 49-56. doi: 10.1109/VR.2016.7504687
- [8] H.H. Ip, and C.S. Chan, (1997, October). Dynamic simulation of human hand motion using an anatomically correct hierarchical approach. In *Systems, Man, and Cybernetics, 1997. Computational Cybernetics and Simulation., 1997 IEEE International Conference on (Vol. 2, pp. 1307-1312). IEEE.*
- [9] H. Ishiyama and S. Kurabayashi, "Monochrome glove: A robust real-time hand gesture recognition method by using a fabric glove with design of structured markers," 2016 IEEE Virtual Reality (VR), Greenville, SC, 2016, pp. 187-188. doi: 10.1109/VR.2016.7504716
- [10] A. H. F. Lam, W. J. Li, Yunhui Liu and Ning Xi, "MIDS: micro input devices system using MEMS sensors," *IEEE/RSJ International Conference on Intelligent Robots and Systems, Lausanne, Switzerland, 2002*, pp. 1184-1189 vol.2. doi: 10.1109/IRDS.2002.1043893
- [11] R. McCall, S. O'Neil, and F. Carroll, *Measuring presence in virtual environments*. ACM, 2004. ID: acm985934; ACM Digital Library; ACM Digital Library (Association for Computing Machinery); KESLI (ACM Digital Library).
- [12] N. O-larnnithipong, A. Barreto, S. Tangnimitchok, N. Ratchatanantakit, "Orientation Correction for a 3D Hand Motion Tracking Interface Using Inertial Measurement Units." *Human-Computer Interaction. Interaction Technologies. Lecture Notes in Computer Science book series*. Vol. 10903. pp. 321-333. Springer (2018).
- [13] M. Slater, M. Usoh, and A. Steed, "Depth of presence in virtual environments," *Presence: Teleoperators & Virtual Environments*, vol. 3, no. 2, pp. 130-144, 1994.
- [14] M. Slater and S. Wilbur, "A framework for immersive virtual environments (Five)," *Presence: Teleoperators & Virtual Environments*, vol. 6, no. 6, p. 603, 1997.
- [15] Rong Zhu and Zhaoying Zhou, "A real-time articulated human motion tracking using tri-axis inertial/magnetic sensors package," in *IEEE Transactions on Neural Systems and Rehabilitation Engineering*, vol. 12, no. 2, pp. 295-302, June 2004. doi: 10.1109/TNSRE.2004.827825